How good is good? Probabilistic benchmarks and nanofinance+

Preprint

Rolando Gonzales Martinez*
Helmholtz-Zentrum Dresden-Rossendorf (Germany) | University of Agder (Norway)
rolando.gonzales@hzdr.de | rolando.gonzales@uia.no

March 3, 2021

Abstract

Benchmarks are standards that allow to identify opportunities for improvement among comparable units. This study suggests a 2-step methodology for calculating probabilistic benchmarks in noisy data sets: (*i*) double-hyperbolic undersampling filters the noise of key performance indicators (KPIs), and (*ii*) a relevance vector machine estimates probabilistic benchmarks with denoised KPIs. The usefulness of the methods is illustrated with an application to a database of nano-finance+. The results indicate that—in the case of nano-finance groups—a higher discrimination power is obtained with variables that capture the macro-economic environment of the country where a group operates. Also, the estimates show that groups operating in rural regions have different probabilistic benchmarks, compared to groups in urban and peri-urban areas.

***K*eywords** benchmarks · nanofinance(+) · KPIs · denoising · relevance vector machines

*This research was carried out with funds provided by the FAHU foundation. The author would like to thank the comments of M. A. Mosashvili.

1 Introduction

Benchmarking is the process of analyzing key performance indicators with the aim of creating standards for comparing competing units (Bogetoft and Otto, 2010). Probabilistic benchmarks measure the probability of a unit falling into an interval along with the cumulative probability of exceeding a predetermined threshold (Wolfe et al., 2019). As a management tool, benchmarks allow to identify and apply better documented practices (Bogetoft, 2013).

Benchmarks are widely used in diverse scientific disciplines. Pharmaceutics compare the prices of prescription drugs with benchmarks (Gencarelli, 2005). In environmental science, benchmarks set water quality standards (Dam et al., 2019) or define thresholds for radiation risk (Bates et al., 2011). In finance, interest-rate benchmarks mitigate search frictions by lowering informational asymmetries in the markets (Duffie, Dworczak, and Zhu, 2017).

This study develops a 2-step processes for calculating probabilistic benchmarks in noisy datasets. In step 1, double-hyperbolic undersampling filters the noise of key performance indicators (KPIs); in step 2, a relevance vector machine estimate probabilistic benchmarks with filtered KPIs. Archimidean copulas approximate the joint density of KPIs during the denoising step. Besides estimating probabilistic benchmarks, the methods of step 2 identify the continuous and categorical factors influencing benchmarks.

The 2-step methodology is illustrated with an application to a database of nanofinance+ working with business interventions. In nanofinance, low-income individuals without access to formal financial services get together and start to accumulate their savings into a fund, which they later use to provide themselves with loans and insurance. In nanofinance+ (NF+), development agencies, donors and governments help communities to create NF+ groups for financial inclusion and then the groups become a platform for additional 'plus' sustainable development programs—see Gonzales Martínez (2019) for details.

The methods proposed in this study complement the state-of-the-art in probabilistic benchmarking of Chakarov and Sankaranarayanan (2014), Chiribella and Adesso (2014) or Yang, Chiribella, and Adesso (2014). Along with this methodological contribution, the empirical findings of this document fill the research gap left by economic studies that have been focused only on calculating benchmarks for microfinance institutions—see for example Tucker (2001) or Reille, Sananikone, and Helms (2002). In microfinance, benchmarks are used to compare institutions; in nanofinance, benchmarks are aimed to compare groups. Benchmarks for nanofinance groups allow to set performance standards for monitoring and evaluating intervention programs implemented in communities worldwide.

The definition of multivariate probabilistic benchmarks used in the study is described in Section 2. Section 3 discusses the methods for estimating multivariate probabilistic benchmarks in noisy datasets. Section 4 shows the empirical application to the NF+ database. Section 5 concludes. The data and the MatLab codes that allow to replicate the results of the study are freely available at MathWorks file-exchange (https://nl.mathworks.com/matlabcentral/fileexchange/74398-double-hyperbolic-undersampling-probabilistic-benchmarks).

2 Multivariate probabilistic benchmarks

Classical benchmarking makes use of fixed inputs to calculate point estimates for classification standards. Probabilistic benchmarking, in contrast, takes into account elements of uncertainty in the inputs and thus generates interval estimates as an output (Liedtke et al., 1998). For example, probabilistic benchmarks are calculated for quantum information protocols—teleportation and approximate cloning—in Yang, Chiribella, and Adesso (2014); more recently, Lipsky et al. (2019) calculate probabilistic benchmarks for noisy anthropometric measures, and Wolfe et al. (2019) use probabilistic benchmarks to quantify the uncertainty in fibromyalgia diagnosis.

Proposition 1 below shows the definition of multivariate probabilistic benchmarks used in this study.

Proposition 1: Multivariate probabilistic benchmarks. *Let* $\mathbf{y}$ *be a* $N \times j$ *matrix* $\mathbf{y} \in \mathbb{R}^j$ *of* j*-KPIs (*$y_1, y_2, ..., y_j$ *key performance indicators) for a set* $\mathcal{H}$ *of* $\{\eta_1, \eta_2, ..., \eta_N\} \ni \mathcal{H}$ *comparable units. Given the joint density,*

$$f_{\mathbf{y}}(\mathbf{y}) := f(y_1, y_2, ..., y_j) = \frac{\partial F(y_1, y_2, ..., y_j)}{\partial y_1 \partial y_2 \cdots \partial y_j},$$

where $F(y_1, y_2, ..., y_j)$ *is a CDF and* $f(y_1, y_2, ..., y_j) \geq 0$*, the differentiated units* $\hbar_\tau \subset \mathcal{H}$ *will be those for which:*

$$1 - \int_{\tau_1}^{\infty} \int_{\tau_2}^{\infty} \cdots \int_{\tau_j}^{\infty} f(y_1, y_2, ..., y_j)\, dy_1 dy_2 \cdots dy_j, \tag{1}$$

given a threshold τ *in* $\tau \in \mathbb{R}^j$*.*

In proposition 1, the discrimination of $\eta_1, \eta_2, ..., \eta_N$ units in a comparable set $\mathcal{H}$ is based on interval estimates of a multi-dimensional threshold (the benchmark) τ. Proposition 1 sets a probabilistic standard based on the joint multivariate distribution function of the KPIs $\{y_1, y_2, ..., y_j\} \ni \mathbf{y}$ used

for calculating τ. The isolines—the contour intervals—defined by the benchmarks τ allow to identify the units $\hbar_\tau$ with a different performance in the unit hypercube ($\hbar_\tau \subset \mathcal{H}$).

Proposition 2 below states that the thresholds τ can be calculated without the need to know the exact form of the joint density $f_{\mathbf{y}}(\mathbf{y})$ in Equation 1:

Proposition 2: Unit-hypercube approximation. *Let $\mathcal{C}_\Theta : [0,1]^d \mapsto [0,1]$ be a d-dimensional multivariate cumulative distribution function with $\mathbf{u} \in \{u_1, u_2, ..., u_d\}$ uniform marginal distributions and a dependence structure defined by Θ. If $\mathbf{u} \equiv F_{\mathbf{y}}(\mathbf{y})$, the joint density of $\mathbf{y}$ needed to calculate τ can be approximated with the simulation of $\mathcal{C}_\Theta(\mathbf{u})$ in the unit hypercube:*

$$\mathcal{C}_\Theta(\mathbf{u}) := \mathcal{C}_\Theta(u_1, u_2, \ldots, u_d) = \int_{-\infty}^{u_1}\int_{-\infty}^{u_2}\cdots\int_{-\infty}^{u_j} c(u_1, u_2, \ldots, u_j)\, du_1 du_2 \cdots du_j,$$

for $\mathcal{C}_\Theta(\mathbf{u}) = 0$ if $u_d = 0$, $\mathcal{C}_\Theta(\mathbf{u}) = u_d$ for any $u_d = 1$, and $\mathcal{C}_\Theta(\cdot)$ satisfies the non-negativity condition on the volume, i.e. $\mathcal{C}_\Theta(\cdot)$ is d-increasing quasi-monotone in $[0,1]^j$.

Proposition 2 is based on Sklar's theorem (Sklar, 1959; Sklar, 1996), which indicates that any multivariate joint distribution can be written in terms of univariate marginal distribution functions and a copulæ $\mathcal{C}_\Theta$ that captures the co-dependence between the variables (Durante, Fernandez-Sanchez, and Sempi, 2013).

Archimidean copulas are a type of copulæ that approximate the joint multivariate distribution of KPIs that are not elliptically distributed (Naifar, 2011). In an Archimedean copula $\mathcal{C}_g$, an additive generation function $g(u)$ models the strength of dependence in arbitrarily high dimensions with only one scalar parameter: θ (Smith, 2003). Formally:

$$\mathcal{C}_g(u_1, u_2, ..., u_d) = \begin{cases} g^{-1}(g(u_1) + g(u_1) + \cdots + g(u_d)) \text{ if } \sum_{v=1}^{d} g(u_v) \leq g(0) \\ 0 \text{ otherwise,} \end{cases} \tag{2}$$

with $g(u)$ a generator function that satisfies $g(1) = 0$, $g'(u) < 0$ and $g''(u) > 0$ for all $0 \leq u \leq 1$; hence $\mathcal{C}_\theta \equiv \mathcal{C}_g$. In Clayton's Archimedean copula, for example, the generator function is equal to $g_\theta(u) = u^{-\theta} - 1$ for $\theta > 1$ (McNeil and Neslehova, 2009; Cherubini et al., 2011):

$$\mathcal{C}_\theta(u_1, u_2, ..., u_d) = \left(1 - d + \sum_{v=1}^{d} u_v^{-\theta}\right)^{-1/\theta}. \tag{3}$$

3 Estimation of multivariate probabilistic benchmarks in noisy datasets

Based on Propositions 1 and 2 above, a 2-step processes is suggested to calculate multivariate probabilistic benchmarks in noisy data sets:

1. In the first step, a swarm algorithm estimates the vector of parameters of a double-hyperbolic noise filter. The optimal estimates of the vector maximize the dependence structure θ in an Archimidean copula calculated with noisy KPIs. The optimal double-hyperbolic filter that maximizes θ is used to denoise the KPIs.

2. In the second step, a relevance vector machine is applied to the denoised KPIs in order to calculate multivariate probabilistic benchmarks. Besides estimating isolines of benchmarks, the relevance vector machine allows to identify factors that influence the benchmarks.

3.1 Step 1: Double-hyperbolic undersampling and swarm optimization

Let $f_h\left(\boldsymbol{\psi}, \mathbf{y}\right)$ be the real $\mathcal{R}$ part—the imaginary part is discarded—of a translated generalized hyperbola of the form (Hamilton and Knop, 1998):

$$f_h\left(\boldsymbol{\psi}, \mathbf{y}\right) := \mathcal{R}\left\{\psi_1\sqrt{\psi_2 + \frac{\psi_3}{\psi_4 + \mathbf{y}}}\right\}, \quad \{\psi_1, \psi_2, \psi_3, \psi_4\} \in \boldsymbol{\psi}, \tag{4}$$

If $f_h^{\perp}\left(\boldsymbol{\psi}^{\perp}, \mathbf{y}\right)$ is an orthogonal/quasi-orthogonal rotation of the translated generalized hyperbola defined by equation 4—with rotation parameters $\left\{\psi_1^{\perp}, \psi_2^{\perp}, \psi_3^{\perp}, \psi_4^{\perp}\right\} \ni \boldsymbol{\psi}^{\perp}$—then the region of the double hyperbola defined by the lobes of $f_h\left(\boldsymbol{\psi}, \mathbf{y}\right)$ and $f_h^{\perp}\left(\boldsymbol{\psi}^{\perp}, \mathbf{y}\right)$ can be used to filter the noise of the joint distribution of $\mathbf{y}$, if elements of $\mathbf{y}$ outside the lobes of $f_h\left(\boldsymbol{\psi}, \mathbf{y}\right)$ and inside the lobes of the rotated hyperbola $f_h^{\perp}\left(\boldsymbol{\psi}^{\perp}, \mathbf{y}\right)$ are discarded.

Let $\mathbf{y}_h \subset \mathbf{y}$ be a vector with the non-discarded elements of $\mathbf{y}$ inside the lobes of $f_h\left(\boldsymbol{\psi}, \mathbf{y}\right)$ and outside the lobes of $f_h^{\perp}\left(\boldsymbol{\psi}^{\perp}, y\right)$. The vector $\mathbf{y}_h$ is an optimal noise reduction of the original data $\mathbf{y}$ if the values of $\boldsymbol{\psi}$ and $\boldsymbol{\psi}^{\perp}$ maximize the dependence structure (θ) of an Archimidean copula estimated with *samples* of $\mathbf{y}$,

$$\max_{\substack{\{\boldsymbol{\psi}, \boldsymbol{\psi}^{\perp}\} \in \mathbb{R} \\ \mathbf{y}_h \subset \mathbf{y}}} \left(-2\int_0^1 \frac{u^{-\theta} - 1}{-\theta u^{-(\theta+1)}}\right)^{-1} - 2\int_0^1 \frac{u^{-\theta} - 1}{-\theta u^{-(\theta+1)}} \tag{5}$$

Box 1 below shows a swarm algorithm proposed to estimate the optimal values of $\boldsymbol{\psi}$ and $\boldsymbol{\psi}^{\perp}$ that maximize θ. The algorithm maximizes the co-dependence in the Archimidean copula by taking

samples of the KPIs contained in $\mathbf{y}$. The structure of the swarm algorithm—separation, alignment, cohesion—is inspired by the BOIDS algorithm of artificial life described in Reynolds (1987).

Box 1. Pseudo-code of the swarm algorithm

Data: $\{y_1, y_2, ..., y_j\} \ni \mathbf{y}$
Result: $\boldsymbol{\psi}$, $\boldsymbol{\psi}^{\perp}$
initialization;
$\delta, M, \theta_0, p_0, , p_0^{\perp}, \zeta, \zeta^*$;
while $m \in \mathbb{Z}_+$ **do**
  $w_\delta = \delta \frac{|p|}{\|p\|}, \quad w_\delta^{\perp} = \delta \frac{|p^{\perp}|}{\|p^{\perp}\|}$;
  for $m \leftarrow 1$ **do**
    random exploration of hyperbola parameters;
    $p_m = p_{m-1} + w_\delta \epsilon, \quad p_m^{\perp} = p_{\perp}^{m-1} + w_\delta^{\perp} \epsilon, \quad \epsilon \sim (0, 1)$;
    hyperbolic undersampling;
    $y_h = f_h(p_m, \mathbf{y}), \quad y_h^{\perp} = f_h^{\perp}(p_m^{\perp}, \mathbf{y}), \quad \{y_h, y_h^{\perp}\} \ni \mathbf{y}_h$;
    copula dependence estimated with filtered m-samples;
    $\hat{\theta}_m = C_\theta(\mathbf{y}_h)$;
  end
  $\hat{\theta}^* = \max \left\{ \hat{\theta}_i \right\}_{i=1}^{m}$ (optimal dependence);
  $p^* = p(\hat{\theta}^*), \quad p^{\perp *} = p^{\perp}(\hat{\theta}^*)$ (optimal hyperbola parameters);
  cohesion = $\frac{1}{2} \left(\|p_m - p_m^*\| + \left\|p_m^{\perp} - p_m^{\perp *}\right\| \right)$;
  separation = $\frac{1}{2} \left(\|p_m - \overline{p}_m^*\| + \left\|p_m^{\perp} - \overline{p}_m^{\perp *}\right\| \right)$;
  if $\hat{\theta}^* > \hat{\theta}^{m-1}$ **then**
    $\hat{\theta}_m = \hat{\theta}^*$;
    $p_m = p^*, \quad p_m^{\perp} = p^{\perp *}$;
    alignment;
    $\delta_m = \delta_{m-1}(\zeta^*)$;
    $m = M - 1$;
  else
    $\delta_m = \delta_{m-1}(\zeta)$;
  end
end

In the swarm algorithm, $\delta, M, \theta_0, p_0, p_0^{\perp}, \zeta, \zeta^*$ are initialization parameters. The parameter $\delta \in \mathbb{R}_+$ controls the initial dispersion of the particles, M is the initial number of particles used to explore possible values of θ; $\theta_0 = 0$ is the starting value of θ_m; $p_0, p_0^{\perp}$ are the starting values of $p_m, p_m^{\perp}$; ζ, ζ^* are parameters that control the degree of exploration in the swarm algorithm. Exploitation (δ) and exploration parameters (ζ, ζ^*) are typical of metaheuristic algorithms in general and swarm intelligence in particular—see for example Tilahun (2019).

The algorithm described in Box 1 explores optimal values of the hyperbola parameters $p_m, p_m^{\perp}$ during m-iterations, based on two behavioral rules: cohesion and separation. Swarm cohesion depends on the euclidean norm between $p_m, p_m^{\perp}$ and the optimal values $p_m^*, p_m^{\perp *}$ calculated with θ^*. Swarm separation is a function of the norm between $p_m, p_m^{\perp}$ and the centroids $\overline{p}_m^*, \overline{p}_m^{\perp *}$. Cohesion abstains the swarm m from including extreme outliers—and thus avoids a biased estimation of θ—and separation guarantees that the swarm properly explores all the potential values that can maximize θ for an optimal noise filtering. Alignment is achieved by gradually reducing exploration and exploitation with ζ^* ($0 < \zeta > \zeta^* \leq 1$).

3.2 Step 2: Relevance vector machines

Traditional methods of supervised learning—as stochastic vector machines—produce point estimates of benchmarks as an output. Relevance vector machines, in contrast, estimate the conditional distribution of multivariate benchmarks in a fully probabilistic framework. Compared to stochastic vector machines, relevance vector machines capture uncertainty and make use of a small number of kernel functions to produce posterior probabilities of membership classification.

Let $\{\mathbf{x}_i\}_{i=1}^k$ be a k-set of covariates influencing the KPIs contained in $\mathbf{y}$. The importance of each covariate is defined by a weight vector $\mathbf{w} = (w_0, \ldots, w_k)$. In a linear approach, $\mathbf{y} = \mathbf{w}^\top \mathbf{x}$. In the presence of a non-linear relationship between $\mathbf{y}$ and $\mathbf{x}$, a nonlinear maping $\mathbf{x} \to \phi(\mathbf{x})$ is a basis function for $\mathbf{y} = \mathbf{w}^\top \phi(\mathbf{x})$.

Given an additive noise ϵ_k, the benchmark targets $\mathbf{t}$ will be,

$$\mathbf{t} = \mathbf{w}^\top \phi(\mathbf{x}) + \epsilon_k, \tag{6}$$

where ϵ_k are independent samples from a mean-zero Gaussian noise process with variance σ^2. Tipping (2000) and Tipping (2001) offer a spare Bayesian learning approach to estimate $\mathbf{w}$ in Equation 6 based on the likelihood of the complete data set,

$$p(\mathbf{t}|\mathbf{w}, \sigma^2) = (2\pi\sigma^2) \exp\left\{-\frac{1}{2\sigma^2}||\mathbf{t} - \Phi\mathbf{w}||^2\right\},$$

where Φ is a $k \times (k+1)$ design matrix $\Phi = [\phi(\mathbf{x}_1), \phi(\mathbf{x}_2), \ldots, \phi(\mathbf{x}_k)]^\top$ and $\phi(\mathbf{x}_i) = [1, \mathcal{K}(\mathbf{x}_i, \mathbf{x}_1), \mathcal{K}(\mathbf{x}_i, \mathbf{x}_2), \ldots, \mathcal{K}(\mathbf{x}_i, \mathbf{x}_k)]^\top$ for a kernel function $\mathcal{K}(\cdot, \cdot)$. In a zero-mean Gaussian prior for $\mathbf{w}$,

$$p(\mathbf{w}|\boldsymbol{\alpha}) = \prod_{i=0}^{k} \mathcal{G}(w_i|0, \alpha_i^{-1}),$$

$\boldsymbol{\alpha}$ is a vector of $k+1$ hyperparameters, and the posterior distribution over the weights is:

$$\begin{aligned} p(\mathbf{w}|\mathbf{t}, \boldsymbol{\alpha}, \sigma^2) &= \frac{p(\mathbf{t}|\mathbf{w}, \sigma^2)p(\mathbf{w}|\boldsymbol{\alpha})}{p(\mathbf{t}|\boldsymbol{\alpha}, \sigma^2)}, \\ &= (2\pi)^{-(k+1)/2}|\boldsymbol{\Sigma}|^{-1/2} \exp\left\{-\frac{1}{2}(\mathbf{w}-\boldsymbol{\mu})^\top \boldsymbol{\Sigma}^{-1}(\mathbf{w}-\boldsymbol{\mu})||^2\right\}, \end{aligned}$$

where $\boldsymbol{\Sigma} = (\sigma^{-2}\boldsymbol{\Phi}^\top\boldsymbol{\Phi} + \mathbf{A})^{-1}$, $\boldsymbol{\mu} = \sigma^{-2}\boldsymbol{\Sigma}\boldsymbol{\Phi}^\top\mathbf{t}$ and $\mathbf{A} = \text{diag}(\alpha_1, \alpha_2, \ldots, \alpha_k)$. Updating methods for α_i are described in Barber (2012). The complete specification of the hierarchical priors—based on the automatic relevance determination of MacKay (1996) and Neal (2012)—can be found in Tipping (2001).

The assignment of an individual hyperparameter α_k to each weight w_k allows to achieve sparsity in the relevance vector machine. As the posterior distribution of many of the weights is peaked around zero, non-zero weights are associated only with 'relevant' vectors, i.e. with the most relevant influencing factors of the probabilistic benchmarks estimated with the denoised KPIs.

4 Empirical application: probabilistic benchmarks in nanofinance+

This section illustrates the methods described in Section 3 with an application to a database of 7830 nanofinance+ groups receiving entepreneurship and business training in 14 African countries: Benin, Burkina Faso, Ethiopia, Ghana, Malawi, Mozambique, Niger, Sierra Leone, South Africa, Sri Lanka, Tanzania, Togo, Uganda and Zambia. Almost all of the groups in the database work with a development agency (94%), and 43% of the groups are located in rural regions.

Table 1 shows descriptive statistics of group-level characteristics and the macro-economic environment of the countries where the groups operate. On average, each member of NF+ contributes around 29 USD of savings to the common fund and receives on average a loan of 22 USD. Despite the low values of savings and loans, returns on savings in the groups are on average 47%, whereas the equity per member is on average equal to 40 USD (Table 1).

Returns on savings (y_1) and equity per member (y_2) are the KPIs used for calculating the benchmarks of NF+ in the empirical application. Hence, $j = 2$, $\mathbf{y} = [y_1 \quad y_2]$, and the joint distribution in

Proposition 1 simplifies to,

$$f_{y_1,y_2}\left(y_1,y_2\right)=f_{y_1|y_2}\left(y_1|y_2\right)f_{y_1|y_2}\left(y_2\right)=f_{y_2|y_1}\left(y_2|y_1\right)f_{y_2|y_1}\left(y_1\right). \tag{7}$$

Successful units—NF+ groups with a higher financial performance—will be those with KPIs delimitied by the isolines of the threshold τ,

$$1-\int_{\tau_1}^{\infty}\int_{\tau_2}^{\infty}f_{y_1,y_2}\left(y_1,y_2\right)dy_1dy_2,$$

for a probabilistic benchmark $\tau\in\{\tau_1\ \ \tau_2\}$, $\tau\in\mathbb{R}^2$.

Following Proposition 2, the joint density of the KPIs (equation 7) is approximated with a bivariate Archimedean copula:

$$\mathcal{C}_g(u_1,u_2)=\begin{cases}g^{-1}(g(u_1)+g(u_2)) \text{ if } g(u_1)+g(u_2)\leq g(0)\\ 0 \text{ otherwise.}\end{cases} \tag{8}$$

Clayton's Archimedean copula is particularly suitable to model the dynamics of nanofinance+. Clayton's copula has greater dependence in the lower tail compared to the upper tail. In the case of NF+, greater lower tail dependence is expected because groups with low equity will have zero or negative returns, while in contrast there is more dispersion in the indicators of groups with higher performance—i.e. some groups show higher equity but low levels of returns due to lower repayment rates, while groups with low equity may have higher returns due to the higher interest rates charged for their loans.

A bivariate Clayton's Archimedean copula for the uniform marginal distributions of returns on savings (u_1) and equity per member (u_2) will be:

$$\mathcal{C}_\theta(u_1,u_2)=g^{-1}(g(u_1)+g(u_2)) \tag{9}$$

$$=(1+u_1^{-\theta}-1+u_2^{-\theta}-1)^{-1/\theta} \tag{10}$$

$$=(u_1^{-\theta}+u_2^{-\theta}-1)^{-1/\theta} \tag{11}$$

with a probability density function,

$$c_\theta(u_1,u_2)=\frac{\partial^2}{\partial u_1\partial u_2}\mathcal{C}_\theta=\frac{1+\theta}{(u_1u_2)^{\theta+1}}(u_1^{-\theta}+u_2^{-\theta}-1)^{-2-\frac{1}{\theta}} \tag{12}$$

and a co-dependence parameter $\theta \in [0, +\infty)$,

$$\theta = \left(-2 \int_0^1 \frac{u^{-\theta} - 1}{-\theta u^{-(\theta+1)}} \right)^{-1} - 2 \int_0^1 \frac{u^{-\theta} - 1}{-\theta u^{-(\theta+1)}}. \tag{13}$$

The parameter θ controls the amount of dependence in $\mathcal{C}_\theta(u_1, u_2)$. When $\theta \to +\infty$ the dependency between u_1 and u_2 approaches comonoticity,

$$\lim_{\theta \to +\infty} \mathcal{C}_\theta(u_1, u_2) = \min(u_1, u_2), \tag{14}$$

while in turn when $\theta \to 0$, u_1 and u_2 become independent:

$$\lim_{\theta \to 0} \mathcal{C}_\theta(u_1, u_2) = u_1 u_2. \tag{15}$$

In the case of returns on savings and equity per member, it is expected that $\theta \to +\infty$, as both financial indicators should show lower tail co-dependence in NF+.

Figure 1 shows indeed that the swarm optimization of θ—using the data of returns on savings and equity per member—leads to a value of $\hat{\theta} = 3.97$. The estimates of the parameters of the hyperbolas for $\hat{\theta}$ are equal to,

$$\hat{\boldsymbol{\psi}} := \left\{ \hat{\psi}_1, \hat{\psi}_2, \hat{\psi}_3, \hat{\psi}_4 \right\} = \{77.42, 0.87, -10.38, -46.51\},$$
$$\hat{\boldsymbol{\psi}}^\perp := \left\{ \hat{\psi}_1^\perp, \hat{\psi}_2^\perp, \hat{\psi}_3^\perp, \hat{\psi}_4^\perp \right\} = \{55.92, 0.67, 2.26, -15.43\}.$$

Figure 2 shows the optimal denoising of the KPIs of NF+ with double-hyperbolic undersampling. The first step discards the values of ROS and EPM outside the lobes of the hyperbole estimated with $\boldsymbol{\psi}$ and inside the lobes of the hyperbole estimated with $\boldsymbol{\psi}^\perp$ (Figures 2b and 2d). The co-dependence between the KPIs before denoising is contaminated with a high number of outliers (Figure 2e). After denoising, the co-dependence in the lower and upper tails of the KPIs is kept but noisy elements are discarded (Figure 2f).

Table 2 and Figure 3 show the results of estimating the relevance vector machine with the denoised KPIs (step 2). In terms of continuous factors influencing the benchmarks, the main covariates affecting the financial benchmarks of NF+ are those related to the macroeconomic environment, mainly GDP growth, poverty, inequality and the percentage of rural population in the country where a NF+ group operates (Table 2). Savings accumulation and loan provision are the main group-level characteristics influencing the financial benchmarks of NF+; this result is expected—because in NF+ the lending channel is the main source of profit generation—and shows the ability of the relevance vector machine to properly detect variables related to financial benchmarks in denoised datasets.

In relation to categorical factors influencing the benchmarks, Figure 3 shows that the probabilistic benchmarks of NF+ are different in rural groups (Figure 3 left) compared to urban groups (Figure 3 right). While both rural and urban groups have a concentration of financial performance in the lower tail of the joint distribution of the KPIs, higher dispersion in the upper tail is observed in rural groups, and hence the isolines of the probabilistic benchmarks are wider for rural groups compared to urban groups.

In the case of urban and peri-urban nano-finance, groups can be classified as successful with a probability higher than 90% (red contour isoline in Figure 3b) when the groups have returns higher than 55% and equity higher than 80 USD per member (Figures 3f). In rural NF+, however, groups that do not show negative returns and have an equity per member higher than 10 USD are classified as successful with a probability higher than 80% (Figures 3c and 3e).

Figure 1: Swarm optimisation of θ in Clay's Archimidean copula. The copula was estimated with the data of returns on savings and equity per member of nanofinance groups. In the graph, the swarm shows greater dispersion at the start of the iterations, but the cohesion and separation of the flock converge after the iteration 15, when the value of the estimate of θ tends to stabilize.

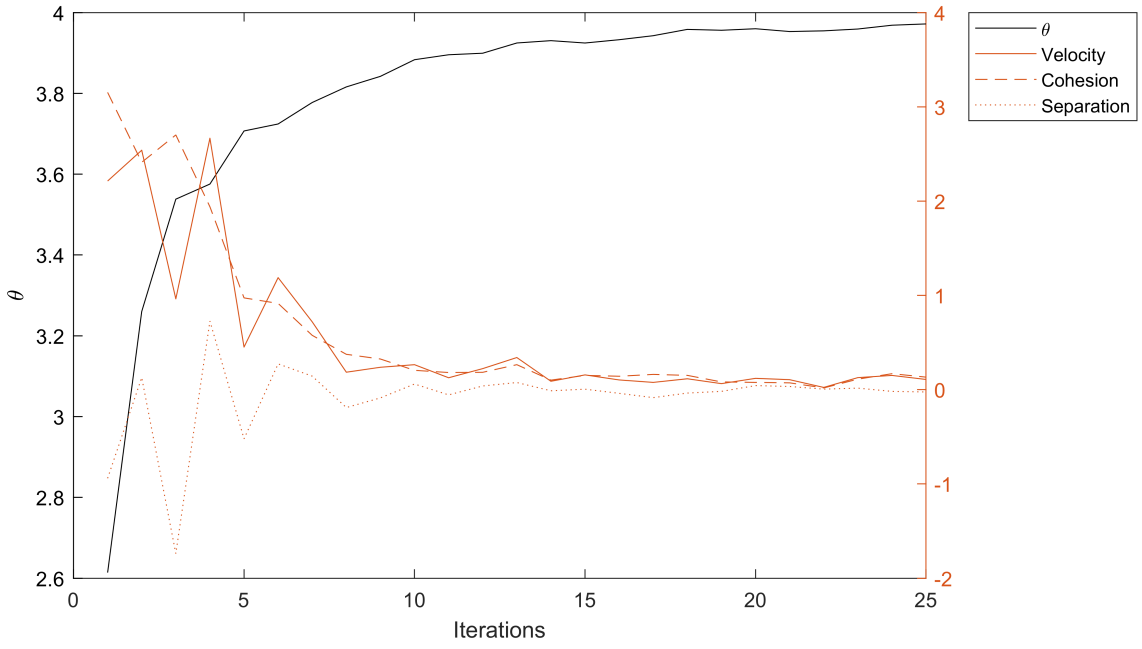

Table 1: Descriptive statistics of the SAVIX. Nanofinance groups in the SAVIX have on average 21 members and 82% of the members are women. The members show a high commitment to the group meetings: member's attendance is 92%, and the members that end up leaving the group are only 1.2% of the total of participants. In macro-economic terms, the GDP growth in the countries where the nanofinance groups operate is on average 4.88%, and the GDP per capita is on average 1353 USD. The countries where the groups are located have also low levels of literacy (the literacy rate is 56%), low levels of financial inclusion (the indicator of financial deepening is 33%), and a high percentage of population living in poverty (40%) and in rural areas (60%).

Variables	**Mean**	**Std. Dev.**	**Min**	**Max**
Group-level characteristics of nanofinance+				
Returns on savings[a]	48.63	47.14	0	199.47
Equity per member[b]	40.41	40.25	0.10	269.90
Savings per member[b]	29.15	28.71	0.06	235.79
Fund utilisation rate[b]	57.73	34.88	0	100.00
Number of loans per member	0.51	0.33	0	1.00
Average loans per member[b]	22.40	29.51	0	186.14
Welfare fund per member[b]	1.32	1.67	0	12.59
Member's attendance[a]	92.32	11.16	39.29	100.00
Drop-out rate[a]	1.17	4.32	0	45.00
Number of members	21.11	6.55	5	33.50
Women members[a]	81.99	23.19	0	100.00
Accumulated loans per member	0.51	0.33	0.00	1.75
Macro-economic variables				
Uncertainty (inflation deviation)[a]	2.87	1.39	0.66	11.54
Inflation rate[a]	6.68	6.88	-1.01	21.87
Age-dependency ratio[a]	87.19	12.91	51.23	111.67
Gini coefficient[a]	45.40	8.10	32.90	63.20
Financial deepening[a]	33.31	31.75	12.55	179.78
Literacy rate[a]	56.24	24.18	15.46	94.37
GDP per capita[b]	1353.04	1410.32	386.73	7575.18
Population density[a]	82.61	54.79	15.12	334.33
Rural population[a]	60.16	13.23	34.15	84.03
Poverty headcount ratio[a]	39.18	11.54	17.70	56.90
GDP growth[a]	4.88	1.61	-1.93	10.25

[a] Percentage (%)
[b] US dollars (USD)

Table 2: Results of estimating the relevance vector machine for $\mathbf{y}$ with the set of covariates $\mathbf{x}$

Type	Covariates ($\mathbf{x}$)	AUC[a]	Gini	Bacc[b]	Prec[c]	FDR[d]
Micro-level characteristics	Savings per member*	1.0000	1.0000	0.9908	1.0000	0.0000
	Fund utilization rate	0.7096	0.4193	0.6326	0.3723	0.6277
	Number of loans per member*	0.8261	0.6522	0.7514	0.6355	0.3645
	Average loans per member*	0.7852	0.5703	0.8716	0.9955	0.0045
	Welfare fund per member*	0.8035	0.6071	0.7675	0.8110	0.1890
	Mmember's attendance	0.6067	0.2134	0.5000	0.0000	1.0000
	Drop-out rate	0.5511	0.1021	0.5149	0.0731	0.9269
	Women members	0.6374	0.2748	0.5155	0.0619	0.9381
	Accumulated loans per member*	0.8261	0.6522	0.7514	0.6355	0.3645
	Rural location*	0.7946	0.5893	0.7946	0.8031	0.1969
Macro-economic variables	Uncertainty (inflation deviation)*	0.7620	0.5241	0.7128	0.5073	0.4927
	Inflation rate	0.5860	0.1721	0.5000	0.0000	1.0000
	Age-dependency ratio*	0.7606	0.5212	0.7836	0.8268	0.1732
	Inequality (Gini index)*	0.8393	0.6785	0.7447	0.5534	0.4466
	Financial deepening	0.7369	0.4739	0.7378	0.5816	0.4184
	Literacy rate	0.6774	0.3548	0.5000	0.0000	1.0000
	GDP per capita*	0.7873	0.5745	0.5011	0.1271	0.8729
	Population density*	0.7939	0.5878	0.7276	0.5748	0.4252
	Rural population in a country*	0.8485	0.6970	0.7532	0.5591	0.4409
	Poverty headcount ratio*	0.8487	0.6973	0.7961	0.7030	0.2970
	GDP growth*	0.8516	0.7031	0.7374	0.6614	0.3386
Facilitation mechanisms of development agencies	No facilitating agency	0.5025	0.0051	0.5000	0.0000	1.0000
	No donors	0.5479	0.0957	0.5000	0.0000	1.0000
	Group formed by paid agent	0.6803	0.3605	0.6803	0.6828	0.3172
	Group formed by field officer	0.5147	0.0295	0.5000	0.0000	1.0000
	Group formed by unpaid agent	0.5264	0.0529	0.5264	0.0754	0.9246
	Group formed by project-paid agent	0.5264	0.0528	0.5264	0.0877	0.9123
	Graduated groups	0.5882	0.1764	0.5000	0.0000	1.0000

(*) Variables with the best machine-learning indicators
[a] AUC: Area under the ROC courve
[b] Bacc: Balanced accuracy
[c] Prec: Precision
[d] FDR: False detection rate

Figure 2: Denoising with double-hyperbolic undersampling. For an optimal filtering of noise, the points outside the lobes of the first hyperbole are discarded in graph (b), and the points inside the lobes of the second hyperbole are discarded in graph (d). Figure (e) shows the relationship between the KPIs before denoising, and figure (f) shows the relation after denoising.

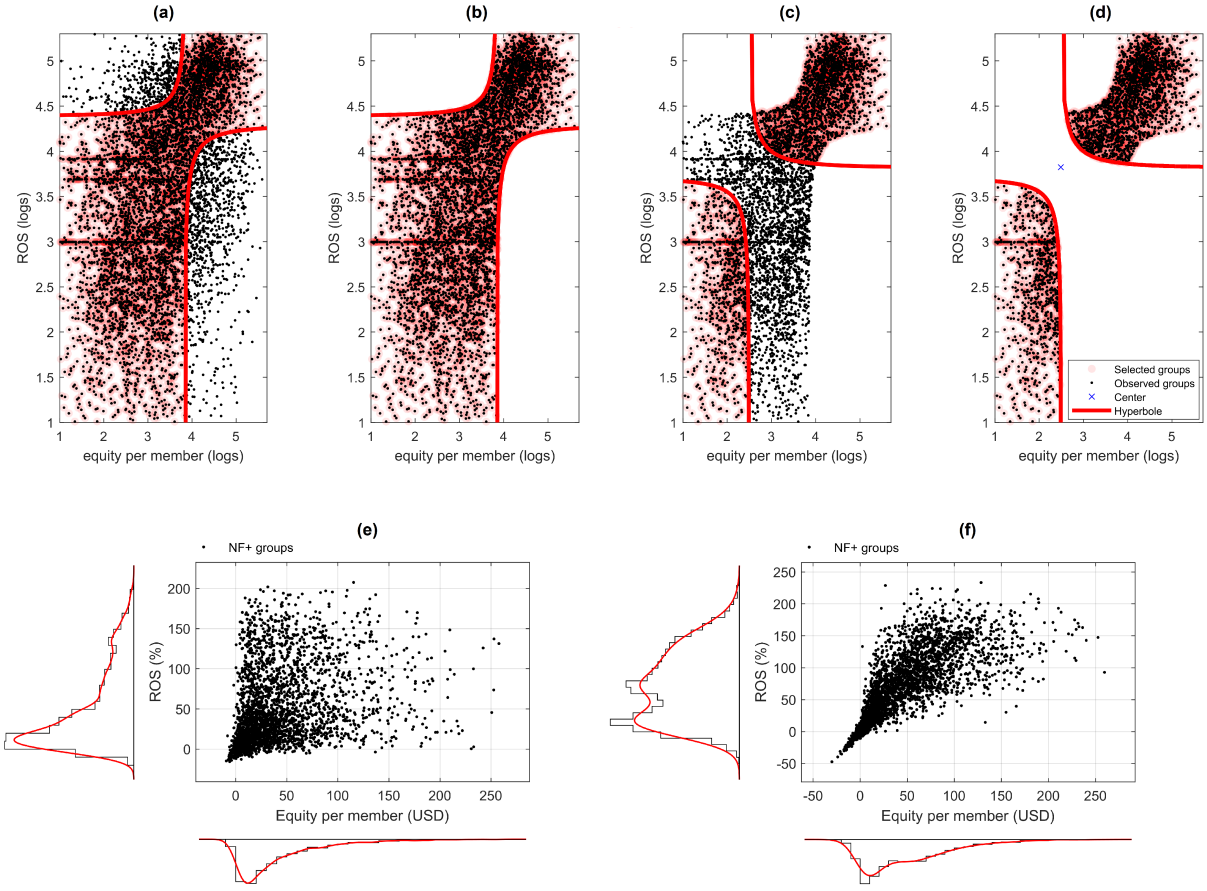

Figure 3: Probabilistic benchmarks estimated with the relevance vector machine

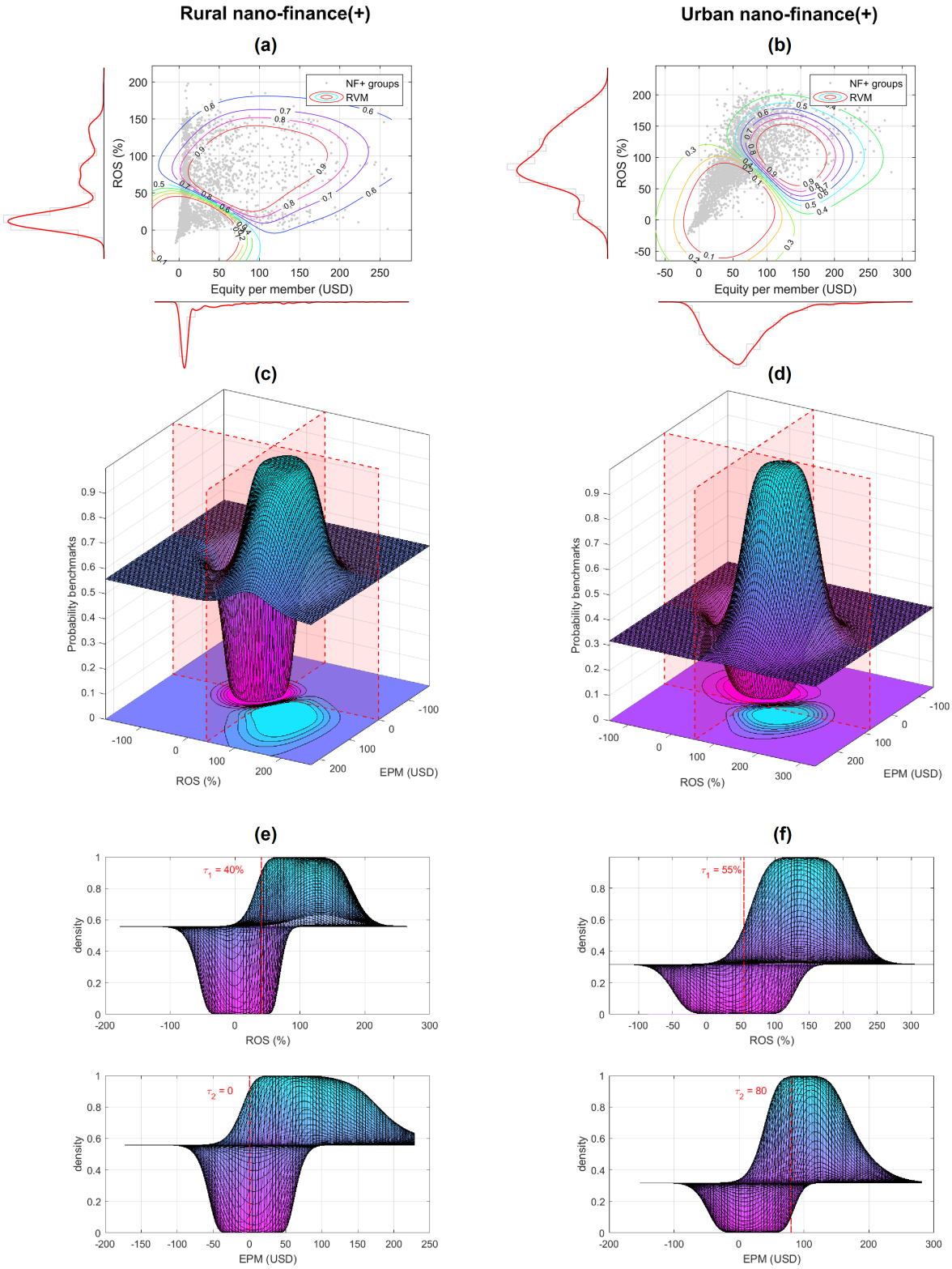

5 Conclusion

This study suggested a 2-step approach for calculating probabilistic benchmarks with noisy KPIs. An empirical application to a noisy database of nanofinance+ shows that the methods are able to denoise KPIs, estimate probabilistic benchmarks, and properly identify the continuous and discrete factors influencing the benchmarks.

In the case of NF+ groups with business training, the results indicate that macroeconomic factors and the region where a group is located influence their financial benchmarks. Governments, international donors and development agencies can use the estimated benchmarks for monitoring the performance of NF+ and gain an independent perspective about how well a group/project is performing when compared to other similar groups/projects. In the presence of performance gaps, the benchmarks will be useful to identify opportunities for change and improvement among the groups[2].

Future studies can extend the denoising methods to the quadratic surface defined by hyperbolic cylinders. The higher-dimensional hierarchical Archimedean copula proposed by Savu and Trede (2010) can be applied to approximate the multivariate probability distribution of KPIs denoised with hyperbolic cylinders. The recent developments in orthogonal machine learning—see *inter alia* Oprescu, Syrgkanis, and Wu (2018), Knaus (2018), Semenova (2018) or Kreif and DiazOrdaz (2019)—can be used to estimate quasi-causal factors influencing the benchmarsk, complementing the non-parametric correlational approach of relevance vector machines.

References

Barber, David (2012). *Bayesian reasoning and machine learning*. Cambridge University Press.

Bates, Matthew E et al. (2011). "Environmental radiation: risk benchmarks or benchmarking risk assessment". In: *Integrated environmental assessment and management* 7.3, pp. 400–403.

Bogetoft, Peter (2013). *Performance benchmarking: Measuring and managing performance*. Springer Science & Business Media.

Bogetoft, Peter and Lars Otto (2010). *Benchmarking with Dea, Sfa, and R*. Vol. 157. Springer Science & Business Media.

Burlando, Alfredo and Andrea Canidio (2017). "Does group inclusion hurt financial inclusion? Evidence from ultra-poor members of Ugandan savings groups". In: *Journal of Development Economics* 128, pp. 24–48.

[2]It is estimated that over 100 million people in 10.5 million households participate in nanofinance groups worldwide (Greaney, Kaboski, and Van Leemput, 2016; Burlando and Canidio, 2017). Due to the importance of NF+ for financial inclusion and multidimensional poverty reduction, all major international donors and development agencies work with NF+, but these organizations lack of benchmarks to evaluate the financial performance of NF+ groups.

Chakarov, Aleksandar and Sriram Sankaranarayanan (2014). "Expectation invariants for probabilistic program loops as fixed points". In: *International Static Analysis Symposium*. Springer, pp. 85–100.

Cherubini, Umberto et al. (2011). *Dynamic Copula methods in finance*. Vol. 625. John Wiley & Sons.

Chiribella, Giulio and Gerardo Adesso (2014). "Quantum benchmarks for pure single-mode Gaussian states". In: *Physical review letters* 112.1, p. 010501.

Dam, Rick A van et al. (2019). "How specific is site-specific? A review and guidance for selecting and evaluating approaches for deriving local water quality benchmarks". In: *Integrated environmental assessment and management* 15.5, pp. 683–702.

Duffie, Darrell, Piotr Dworczak, and Haoxiang Zhu (2017). "Benchmarks in search markets". In: *The Journal of Finance* 72.5, pp. 1983–2044.

Durante, Fabrizio, Juan Fernandez-Sanchez, and Carlo Sempi (2013). "A topological proof of Sklar's theorem". In: *Applied Mathematics Letters* 26.9, pp. 945–948. ISSN: 0893-9659.

Gencarelli, DM (2005). "One pill, many prices: variation in prescription drug prices in selected government programs." In: *Issue brief (George Washington University. National Health Policy Forum: 2005)*. 807, p. 1.

Gonzales Martínez, Rolando (2019). "Which social program supports sustainable grassroot finance? Machine-learning evidence". In: *International Journal of Sustainable Development & World Ecology*, pp. 1–7.

Greaney, Brian P, Joseph P Kaboski, and Eva Van Leemput (2016). "Can self-help groups really be "self-help"?" In: *The Review of Economic Studies* 83.4, pp. 1614–1644.

Hamilton, David C and O Knop (1998). "Combining non-linear regressions that have unequal error variances and some parameters in common". In: *Journal of the Royal Statistical Society: Series C (Applied Statistics)* 47.2, pp. 173–185.

Knaus, Michael C (2018). "A Double Machine Learning Approach to Estimate the Effects of Musical Practice on Student's Skills". In: *arXiv preprint arXiv:1805.10300*.

Kreif, Noemi and Karla DiazOrdaz (2019). "Machine learning in policy evaluation: new tools for causal inference". In: *arXiv preprint arXiv:1903.00402*.

Liedtke, Jochen et al. (1998). "Irreproducible benchmarks might be sometimes helpful". In: *Proceedings of the 8th ACM SIGOPS European workshop on Support for composing distributed applications*, pp. 242–246.

Lipsky, Leah M et al. (2019). "Accuracy of self-reported height, weight, and BMI over time in emerging adults". In: *American journal of preventive medicine* 56.6, pp. 860–868.

MacKay, David JC (1996). "Bayesian methods for backpropagation networks". In: *Models of neural networks III*, pp. 211–254.

McNeil, Alexander J. and Johanna Neslehova (2009). "Multivariate Archimedean Copulas, d-Monotone Functions and L1-Norm Symmetric Distributions". In: *The Annals of Statistics* 37.5B, pp. 3059–3097.

Naifar, Nader (2011). "Modelling dependence structure with Archimedean copulas and applications to the iTraxx CDS index". In: *Journal of Computational and Applied Mathematics* 235.8, pp. 2459–2466.

Neal, Radford M (2012). *Bayesian learning for neural networks*. Vol. 118. Springer Science & Business Media.

Oprescu, Miruna, Vasilis Syrgkanis, and Zhiwei Steven Wu (2018). "Orthogonal random forest for causal inference". In: *arXiv preprint arXiv:1806.03467*.

Reille, Xavier, Ousa Sananikone, and Brigit Helms (2002). "Comparing microfinance assessment methodologies". In: *Small Enterprise Development* 13.2, pp. 10–19.

Reynolds, Craig W (1987). "Flocks, herds and schools: A distributed behavioral model". In: *ACM SIGGRAPH computer graphics*. Vol. 21. 4. ACM, pp. 25–34.

Savu, Cornelia and Mark Trede (2010). "Hierarchies of Archimedean copulas". In: *Quantitative Finance* 10.3, pp. 295–304.

Semenova, Vira (2018). "Essays in econometrics and machine learning". PhD thesis. Massachusetts Institute of Technology.

Sklar, Abe (1959). "Fonctions de reprtition an dimensions et leursmarges". In.

– (1996). "Random variables, distribution functions, and copulas: a personal look backward and forward". In: *Lecture notes-monograph series*, pp. 1–14.

Smith, Murray D (2003). "Modelling sample selection using Archimedean copulas". In: *The Econometrics Journal* 6.1, pp. 99–123.

Tilahun, Surafel Luleseged (2019). "Balancing the Degree of Exploration and Exploitation of Swarm Intelligence Using Parallel Computing". In: *International Journal on Artificial Intelligence Tools* 28.03, p. 1950014.

Tipping, Michael E (2000). "Sparse kernel principal component analysis". In: *Advances in neural information processing systems*, pp. 633–639.

– (2001). "Sparse Bayesian learning and the relevance vector machine". In: *Journal of machine learning research* 1.Jun, pp. 211–244.

Tucker, Michael (2001). "Financial performance of selected microfinance institutions: Benchmarking progress to sustainability". In: *Journal of Microfinance/ESR Review* 3.2, p. 7.

Wolfe, Frederick et al. (2019). "Diagnosis of fibromyalgia: Disagreement between fibromyalgia criteria and clinician-based fibromyalgia diagnosis in a university clinic". In: *Arthritis care & research* 71.3, pp. 343–351.

Yang, Yuxiang, Giulio Chiribella, and Gerardo Adesso (2014). “Certifying quantumness: benchmarks for the optimal processing of generalized coherent and squeezed states”. In: *Physical Review A* 90.4, pp. 042319–1.